ADVANCED MATERIALS
www.advmat.de

Attractive Pickering Emulsion Gels

Baiheng Wu, Chenjing Yang, Qi Xin, Linlin Kong, Max Eggersdorfer, Jian Ruan, Peng Zhao, Jianzhen Shan, Kai Liu, Dong Chen, David A. Weitz, and Xiang Gao**

Properties of emulsions highly depend on the interdroplet interactions and, thus, engineering interdroplet interactions at molecular scale are essential to achieve desired emulsion systems. Here, attractive Pickering emulsion gels (APEGs) are designed and prepared by bridging neighboring particle-stabilized droplets via telechelic polymers. In the APEGs, each telechelic molecule with two amino end groups can simultaneously bind to two carboxyl functionalized nanoparticles in two neighboring droplets, forming a bridged network. The APEG systems show typical shear-thinning behaviors and their viscoelastic properties are tunable by temperature, pH, and molecular weight of the telechelic polymers, making them ideal for direct 3D printing. The APEGs can be photopolymerized to prepare APEG-templated porous materials and their microstructures can be tailored to optimize their performances, making the APEG systems promising for a wide range of applications.

1. Introduction

Emulsion gels of one phase dispersed in another enable the design of two-phase systems, where the microstructures and viscoelastic properties can be tailored, and provide an indispensable platform for the preparation of functional materials widely used in material science,[1,2] pharmaceutics,[3,4] and chemical engineering.[5–8] Emulsion gels combine the virtues of both emulsions and gels. While emulsions are generally unstable and tend to revert to separated water and oil phases over time, emulsion gels are stable against droplet coalescence, Ostwald ripening, and phase separation.[9] Emulsion gels also possess various interesting viscoelastic properties, endowing them suitable for many scenarios. The investigations of emulsion gels with tunable microstructures and viscoelastic properties have drawn growing interest.[10,11]

The properties of emulsion gels are strongly influenced by interdroplet interactions and thus engineering interdroplet interactions at molecular scale are essential to achieve desired emulsion gel systems.[12,13] The interdroplet interactions could be repulsive or attractive.[14] When repulsive forces are introduced by, e.g., electrostatic repulsions, the systems require a high volume fraction of the dispersed phase to form stable emulsion gels, usually larger than 0.7.[15,16] The repulsive forces among crowded droplets will kinetically trap droplets in 3D space and the systems cannot flow without external forces, manifesting viscoelastic behaviors.[17] Recently, emulsion gels based on attractive interactions between neighboring droplets have been demonstrated.[18] Attractive interactions between neighboring oil droplets result in strong aggregation of oil droplets into fractal clusters, eventually forming a cross-linked network.[19–21] However, these examples are only limited to oil-in-water emulsion gels. Engineering interdroplet interactions of water-in-oil emulsions is still a great challenge due to the apolar continuous oil phase and thus the preparation of water-in-oil emulsion gels is merely reported, which strongly limits their applications. Innovations of new strategies to precisely engineer interdroplet interactions at a molecular level are essential.

Here, we introduce attractive interactions between neighboring particle-stabilized water droplets and design attractive Pickering emulsion gels (APEGs) by bridging them via telechelic polymers. The water droplets are covered and stabilized by negatively-charged nanoparticles (NPs), which also provide active sites for the electrostatic binding of positively-charged telechelic polymers. Each positively-charged telechelic molecule could simultaneously bind to two negatively-charged NPs in two neighboring water droplets, thus bridging

Dr. B. Wu, Prof. J. Ruan, Prof. P. Zhao, Prof. J. Shan, Prof. D. Chen
Department of Medical Oncology
The First Affiliated Hospital
School of Medicine
Zhejiang University
Hangzhou 310003, P. R. China
E-mail: chen_dong@zju.edu.cn

Dr. B. Wu, C. Yang, Q. Xin, L. Kong, Prof. D. Chen, Prof. X. Gao
College of Energy Engineering
Zhejiang University
Hangzhou 310027, P. R. China
E-mail: xgao@zju.edu.cn

Dr. M. Eggersdorferd
Independent Researcher
Zürich 8092, Switzerland

Dr. M. Eggersdorferd, Prof. D. A. Weitz
John A. Paulson School of Engineering and Applied Sciences
Harvard University
Cambridge, MA 02138, USA

Prof. K. Liu
Department of Chemistry
Tsinghua University
Beijing 100084, P. R. China

The ORCID identification number(s) for the author(s) of this article can be found under https://doi.org/10.1002/adma.202102362.

DOI: 10.1002/adma.202102362

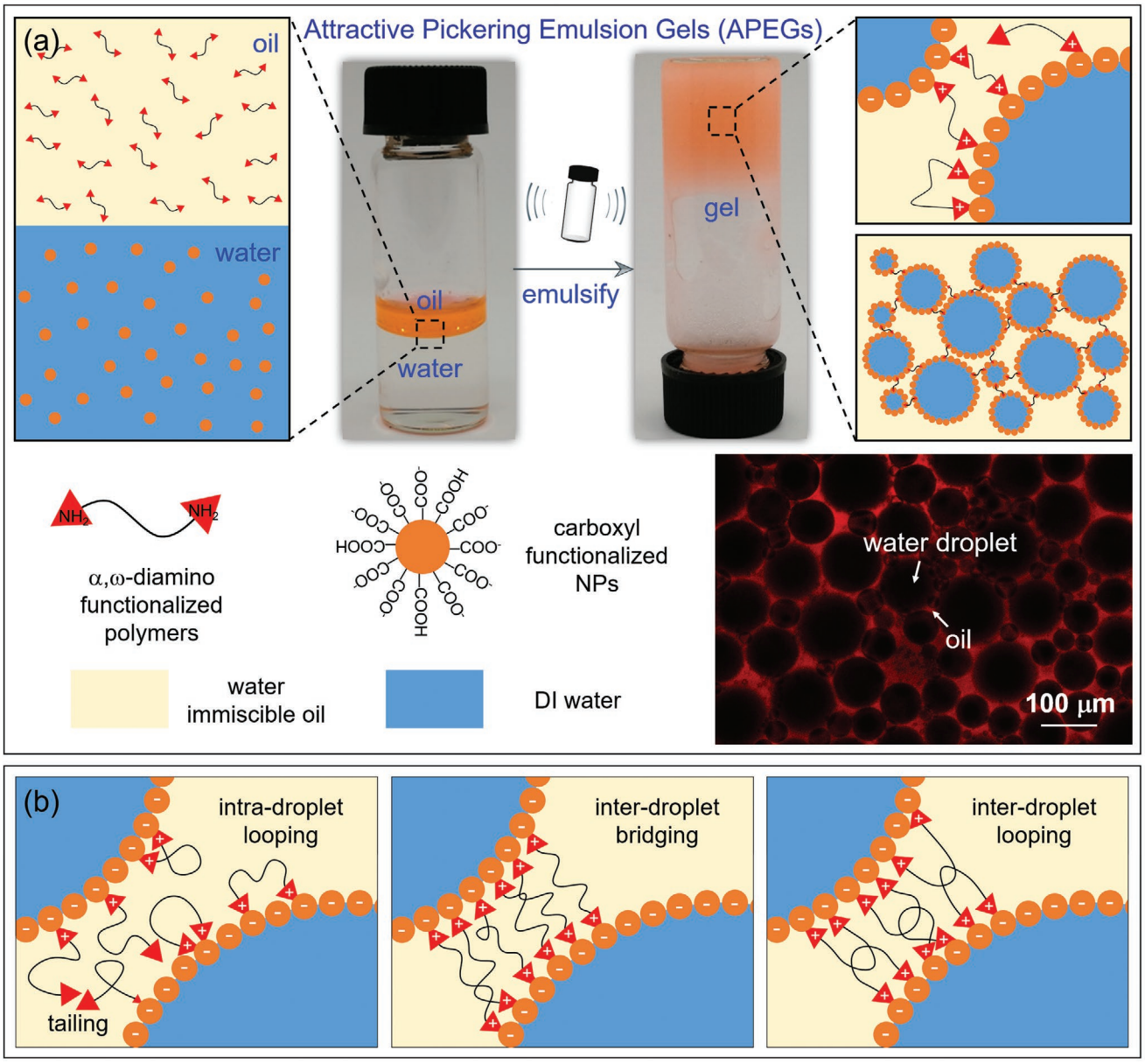

Figure 1. Attractive Pickering emulsion gels (APEGs). a) The molecular surfactants, α,ω-diamino functionalized polymers, and the colloidal surfactants, carboxyl functionalized NPs, are previously dispersed in the oil and water phases, respectively. When the water phase is emulsified in the oil phase, both molecular and colloidal surfactants go to the water/oil interface, at which negatively-charged NPs electrostatically bind with positively-charged polymers. Diamino functionalized polymers could thus bridge neighboring droplets, forming APEGs. The scenario is confirmed by the fluorescent confocal microscope image of the APEG system, in which the oil phase is dyed with Nile Red. b) Electrostatic complexation between negatively-charged NPs and positively-charged polymers at the interface, including tailing, intradroplet looping, interdroplet bridging and interdroplet looping. Only interdroplet bridging and interdroplet looping contribute to the formation of APEGs.

neighboring droplets and forming APEGs. The APEGs are applicable to various systems and the types of nanoparticles, telechelic polymers, and oil phases are customizable. The shear-thinning viscoelastic properties of the APEGs enable the 3D printing of APEGs directly in air and under water. By tuning the microstructures and mechanical properties, the porous materials prepared using APEGs as templates show superior thermal insulation performances. The APEGs thus present a versatile platform for the development of various functional materials.

2. Results and Discussions

2.1. APEGs

APEGs are prepared by emulsifying the water phase in the oil phase and bridging particle-stabilized water droplets through telechelic polymers, as schematically illustrated in **Figure 1**a. Shellac NPs, an FDA approved natural resin, are prepared by flash nanoprecipitation[22] and dispersed in water. α,ω-diamino functionalized polydimethylsiloxane (NH_2-PDMS-NH_2) polymers

are dissolved in the silk oil phase. Both shellac NPs and NH_2-PDMS-NH_2 polymers are amphiphilic; shellac NPs contain both hydrophobic polyesters and hydrophilic carboxyl groups,[23] while NH_2-PDMS-NH_2 polymers consist of one hydrophobic PDMS backbone and two hydrophilic amino end groups. During the emulsification process, both shellac NPs and telechelic polymers tend to adsorb at the water/oil interface to reduce the interfacial energy. Because the carboxyl groups of shellac NPs are negatively charged and the amino end groups of NH_2-PDMS-NH_2 polymers are positively charged, one amino end group can electrostatically bind to one carboxyl group and each NH_2-PDMS-NH_2 molecule with two amino end groups can simultaneously bind to two shellac NPs in two neighboring droplets, thus performing as a chelator, as modeled in Figure 1b. When the oil phase is dyed with Nile Red, the network of bridged water droplets in the oil phase is directly visualized in the fluorescent confocal microscope image. To confirm the important role of α,ω-diamino functionalized polymers, which bridge neighboring particle-stabilized water droplets and thus contribute to the gelation of water-in-oil emulsions, a series of control experiments are carried out, as shown in Figure S1, Supporting Information. None of the systems with only carboxyl functionalized NPs, with only α,ω-diamino functionalized polymers or with carboxyl functionalized NPs and monoamino functionalized polymers forms Pickering emulsion gels. The electrostatic complexation of carboxyl functionalized NPs and α,ω-diamino functionalized polymers at the water/oil interface is further confirmed by directly observing the thin film formed with SEM images, as shown in Figure S2, Supporting Information.

2.2. Attractive Interactions of APEGs

To investigate the interfacial behaviors of shellac NPs and NH_2-PDMS-NH_2 polymers, the interfacial tensions are monitored over time in the presence of only shellac NPs in water, only NH_2-PDMS-NH_2 polymers in the oil phase or both shellac NPs and NH_2-PDMS-NH_2 polymers, as shown in **Figure 2**a. Both shellac NPs and NH_2-PDMS-NH_2 polymers are amphiphilic, which preferentially adsorb at the water/oil interface. Though shellac NPs could lower the interfacial tension to a lower value of 10 mN m^{-1}, NH_2-PDMS-NH_2 polymers possess larger mobility and thus more rapid adsorption kinetics, essentially lowering the interfacial tension within 1 s. Therefore, the APEG systems preferentially form water-in-oil emulsions even when the water phase is dominant with a volume ratio up to 90%. The presence of both shellac NPs and NH_2-PDMS-NH_2 polymers accompanied by the electrostatic complexations between them facilitates the quick capture of shellac NPs at the interface and prevents the desorption of NH_2-PDMS-NH_2 molecules, displaying both kinetical and thermodynamical advantages in stabilizing the interface. The electrostatic interactions between shellac NPs and NH_2-PDMS-NH_2 polymers are irreversible, which form a thin film at the interface.[24–27] Therefore, when the dispersed phase is withdrawn from a pendent droplet, the buckling of the interface is clearly observed, as shown in Figure 2b.

Direct measurements of the attractive forces between two freshly prepared water droplets are shown in Figure 2c; and Movie S1, Supporting Information. As the bottom droplet slowly approaches and squeezes the top droplet, the effective weight of the top droplet slowly decreases. Once the repulsive force reaches −9.8 μN, the bottom droplet starts to retract from the top droplet and the effective weight of the top droplet increases. During the squeezing and detaching process, intradroplet electrostatic complexations of shellac NPs and NH_2-PDMS-NH_2 polymers at the interface prevent the bottom and top droplets from coalescence, as shown in Figure S3, Supporting Information. Meanwhile, interdroplet attractive interactions gradually develop at the contact region, where telechelic NH_2-PDMS-NH_2 polymers bridge the bottom and top droplets. At the point of detaching, the attractive forces pull down the top droplet and contribute to the abrupt jump in the effective weight of the top droplet. An attractive force of ≈2 μN is obtained from the weight measurement and a detaching work of ≈1.2 ± 0.7 nJ is achieved by integrating the region enclosed by the red fitting curves from four parallel experiments. The attractive forces between freshly prepared water droplets are strong enough to pick up small droplets, for example with a volume of ≈0.2 μL, as shown in Figure 2d; and Movie S2, Supporting Information.

Because of the attractive forces developed between neighboring droplets, emulsified water droplets form an interconnected network, eventually leading to the gelation of APEG systems. Therefore, APEGs form at the bottom of the vials with excess oil phase on the top even when the water phase only has a very low volume fraction of 20%, which is unachievable in systems of high internal phase emulsions.[28,29] The phase diagram of the APEG systems prepared using 20% water is shown in Figure 2e. A minimum concentration of shellac NPs of 0.21 mg mL^{-1} and a minimum concentration of NH_2-PDMS-NH_2 polymers of 1.25 mg mL^{-1} are required for the build-up of attractive forces between neighboring water droplets to ensure successful gelation. If the water volume fraction increases to 80%, the whole system forms stable APEGs without any excess oil phase, as shown in Figure S4, Supporting Information.

2.3. Viscoelastic Properties of APEGs

As mentioned above, APEGs form at the bottom of the vials with excess oil phase on the top due to attractive interactions when the volume fractions of dispersed water droplets are very low, as shown in **Figure 3**a. Interestingly, the APEG systems formed at the bottom have a constant volume fraction of ≈70%, which is slightly larger than that of closely packed polydisperse spherical droplets and is independent of the droplet size, as shown in Figure 3b,c. To get a better understanding of the APEG systems, we systematically investigate the viscoelastic properties of APEGs with an average droplet diameter of D≈15 μm and D≈30 μm, which are prepared by homogenizing and shaking, respectively. The detailed strain sweeps and frequency sweeps of the systems are shown in Figure 3d,e, respectively. Without any shearing, the elastic modulus G' of the APEG systems is approximately one order of magnitude larger than the viscous modulus G'', which is a characteristic feature of stable gels. As the strain applied to the systems gradually increases, the elastic modulus G' gradually decreases while the viscous modulus G'' gradually increases. At strain≈100%, the

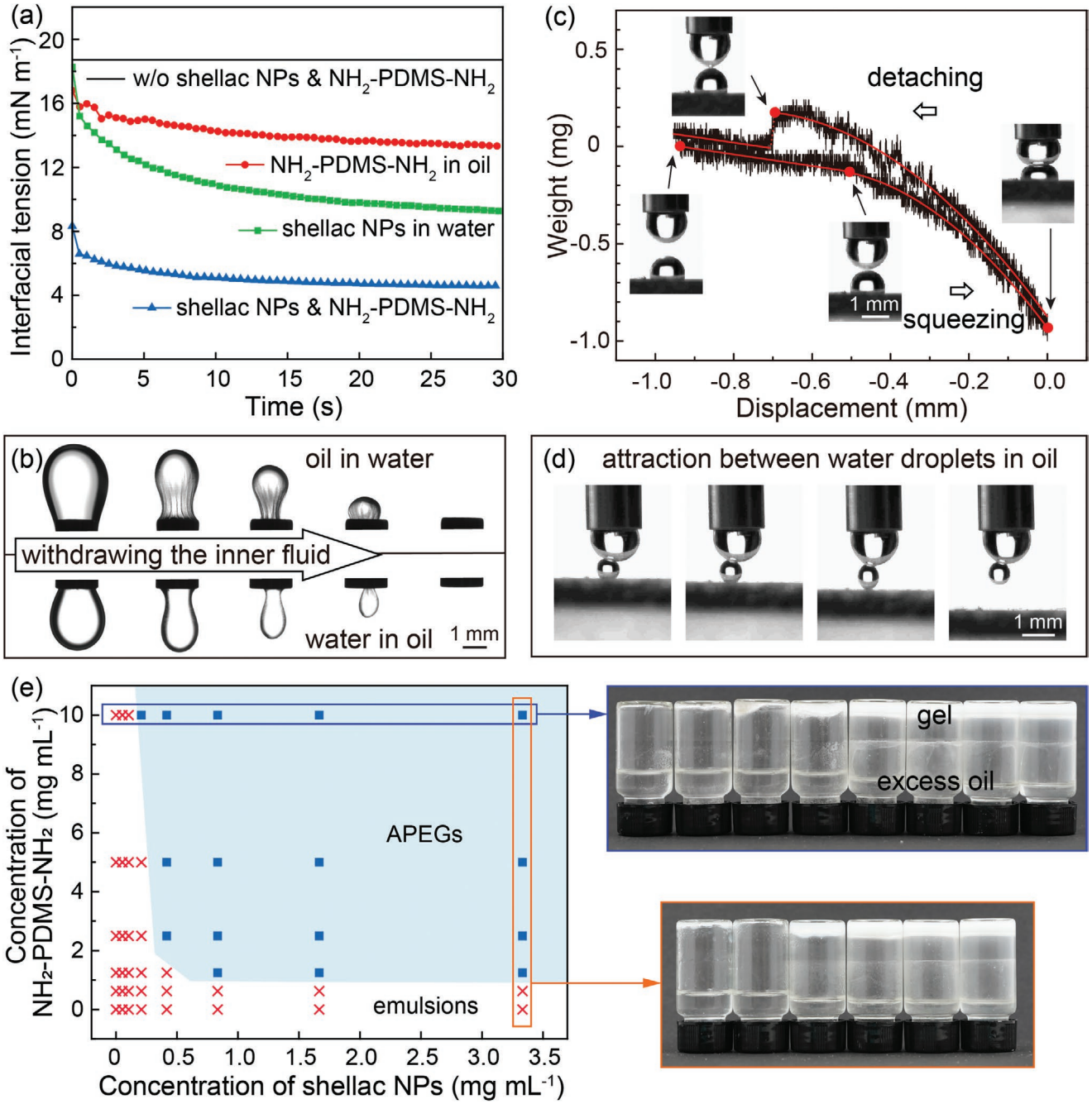

Figure 2. Attractive interactions between particle-stabilized emulsions. a) Dynamic interfacial tensions of water-in-oil droplets under different conditions. If not specified, the concentration of shellac NPs in water is 0.83 mg mL^{-1} and the concentration of NH_2-PDMS-NH_2 in the silk oil phase is 10 mg mL^{-1}. b) Two sequences of snapshots showing the interfacial jamming and buckling when withdrawing the inner fluid due to the electrostatic complexations at the interface. c) Measurements of the attractive forces between two water droplets in the silk oil phase. Insets are the experimental snapshots. d) Picking and lifting of a water droplet via attractive interactions. e) Phase diagram of APEGs prepared by different concentrations of shellac NPs in water and NH_2-PDMS-NH_2 polymers in the silk oil phase. The volume fraction of water is kept constant at 20%. APEGs form at the bottom of the vials with excess oil phase on the top.

viscous modulus G'' becomes larger than the elastic modulus G' at the yield point and fluidity starts to dominate over elasticity in the APEG systems, showing typical shear-thinning behaviors. Compared with APEGs with an average droplet diameter of D≈30 µm, APEGs with an average droplet diameter of D≈15 µm and thus an emulsion network with a higher density of interdroplet bridges show a higher elastic modulus and yield point, as shown in Figure 3f.

In addition to droplet size, the elastic modulus G', viscous modulus G'' and yield point of APEGs can easily be tuned by temperature and pH, as shown in Figure 3g,h, respectively. As the temperature increases, molecular mobility increases

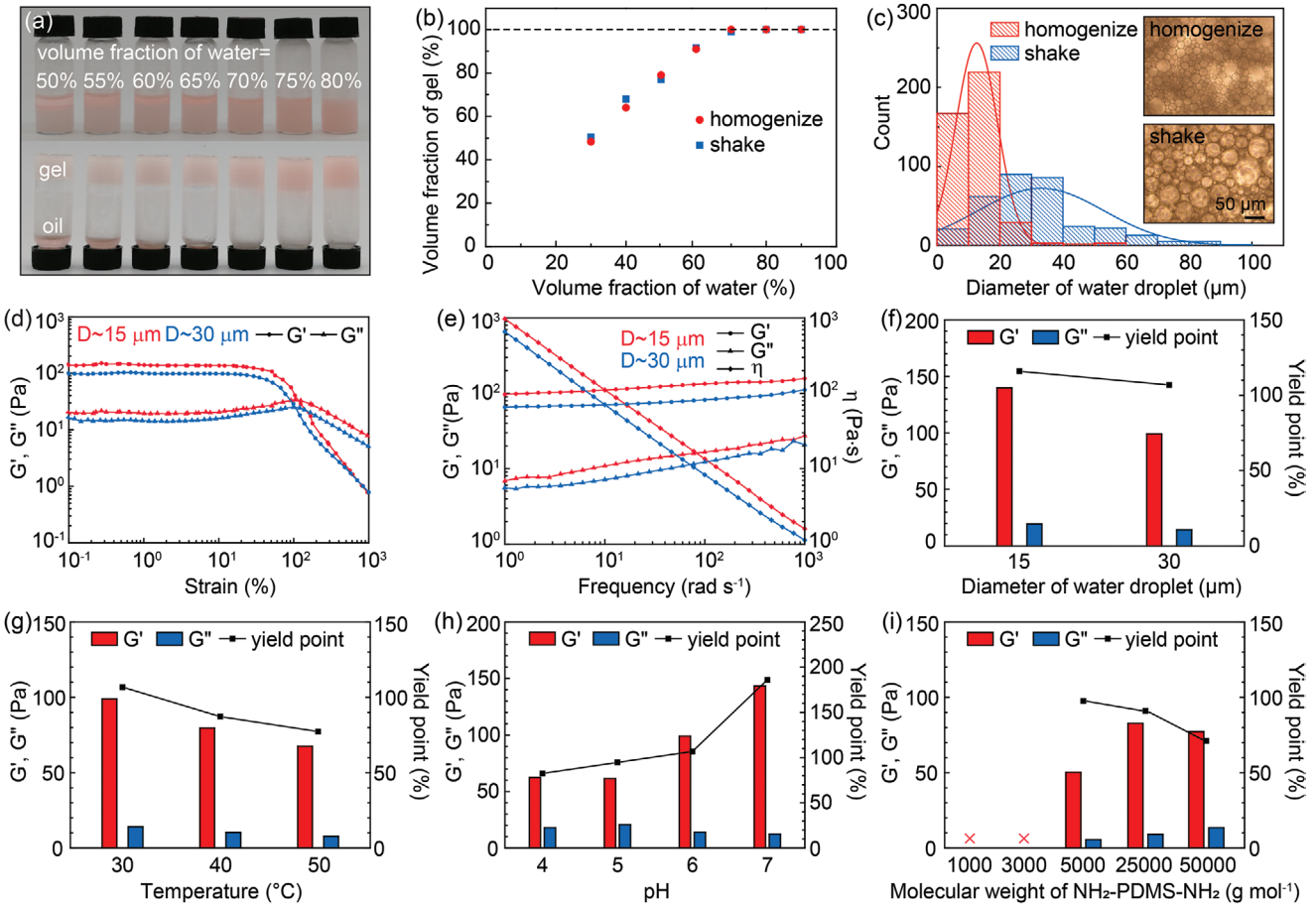

Figure 3. Viscoelastic properties of APEGs and their tunability. a) Images of APEGs prepared using different volume fractions of water. When the volume fraction of water is more than 70%, there is no excess oil phase on top of the APEGs. b) Volume fraction of APEGs as a function of the volume fraction of water, suggesting that the volume fraction of water in the APEGs is constant at ≈70% when the volume fraction of water is less than 70%. If not specified, 1:4 oil-to-water ratio is used to avoid excess oil phase. c) Size distributions of water droplets prepared by shaking and homogenizing, respectively. d) Strain sweeps of elastic modulus G' and viscous modulus G'' of APEGs with different droplet sizes, showing characteristic shear-thinning behaviors. The frequency is kept constant at 10 rad s^{-1}. e) Frequency sweeps of elastic modulus G', viscous modulus G'' and viscosity η. The stress is kept constant at 1 Pa. Dependence of elastic modulus G', viscous modulus G'' and yield point of APEGs on f) droplet diameter, g) temperature, h) pH, and i) molecular weight of NH_2-PDMS-NH_2. × denotes no APEGs.

and the elastic modulus G' of the APEGs slightly decreases, as shown in Figure S5, Supporting Information. The pH condition of the aqueous phase has effects on the electrostatic interaction between shellac NPs and NH_2-PDMS-NH_2. Carboxylic groups on the surface of shellac NPs are weak acids, while amino groups at the two ends of NH_2-PDMS-NH_2 are weak bases. Between pH = 4 and 7, the deprotonation of carboxylic groups on the surface of shellac NPs is the dominant factor, which affects the electrostatic interaction.[30] When the pH increases from pH = 4 to pH = 7, more carboxyl groups on the surface of shellac NPs are deprotonated, which is characterized by the increase of Zeta potential from −30 to −53 mV, as shown in Figure S6a, Supporting Information; therefore, the electrostatic interactions between negatively-charged shellac NPs and positively-charged NH_2-PDMS-NH_2 polymers are strengthened, leading to the increase of the elastic modulus G', as shown in Figure S6b, Supporting Information.

Because the telechelic NH_2-PDMS-NH_2 polymers play an important role in bridging the droplet network, systematic studies on their molecular weight are carried out, as shown in Figure 3i. When the molecular weight of NH_2-PDMS-NH_2 polymers is too small, e.g., M_w = 1000 or 3000 g mol^{-1}, the polymers are too short to form effective interdroplet bridging and looping and there are no APEGs, as shown in Figure S7, Supporting Information. When the molecular weight is large enough, e.g., M_w = 5000 g mol^{-1} with an extended molecular length of ≈17 nm, such systems could form stable APEGs. Generally, the end-to-end distance of NH_2-PDMS-NH_2 molecules increases as their molecular weight increases. Therefore, more telechelic NH_2-PDMS-NH_2 molecules form bridges spanning two neighboring droplets when the molecular weight increases[31] and the elastic modulus G' is expected to increase. However, when the molecular weight of NH_2-PDMS-NH_2 increases from M_w = 25 000 g mol^{-1} to M_w = 50 000 g mol^{-1}, the elastic modulus G' barely changes, as shown in Figure S8, Supporting Information. This is because telechelic polymers with a larger molecular weight adsorbed on a single droplet will lead to stronger resistance against compression and contact between two

neighboring droplets, though more telechelic molecules can form bridges spanning two neighboring droplets.

2.4. 3D Printing of APEGs

The preparation of APEGs is versatile; for oil phases including silk oil, lavender essential oil, n-hexane, styrene monomer, and *n*-butyl acrylate monomer, NPs in water including shellac NPs and carboxyl functionalized silica NPs and telechelic polymers including NH_2-PDMS-NH_2 and NH_2-PS-NH_2, stable APEGs form, as shown in Figure S9, Supporting Information. The APEG systems exhibit excellent stability over a wide temperature range from 4 to 50 °C. Even when the APEGs are destroyed at −20 °C due to ice crystallization, the attractive interactions are redeveloped by shearing at room temperature, forming stable APEGs again, as shown in Figure S10, Supporting Information. The APEGs can also withstand high centrifugal forces and survive over 5000 rpm, as shown in Figure S11, Supporting Information. Though some oil phase may be squeezed out by compressing the water droplets under high centrifugal forces, the systems will recover after relaxation for 4 h, as shown in Figure S12, Supporting Information.

The excellent performances and unique viscoelastic properties of the APEG systems enable the facile processing and customized design of functional materials by direct 3D printing,[32–34] as shown in Figure S13, Supporting Information. Under shearing, the APEGs can continuously be extruded out of the nozzle with the viscous modulus G'' larger than the elastic modulus G'. After leaving the nozzle, the APEGs can quickly recover their viscoelastic property, having the elastic modulus G' larger than the viscous modulus G'' and thus maintaining the printed 3D architectures. The shear-thinning viscoelastic properties make the APEGs ideal for 3D printing inks, which are directly printed into 2D patterns and 3D architectures by a customized 3D printer, as shown in **Figure 4**a,b, respectively. Since the APEG systems mainly consist of bridged water droplets in the oil phase, the APEGs are also feasible for underwater 3D printing, such as the Snow White and Pool Tower, as shown in Figure 4c,d, respectively. After removing the outer water media, the 3D printed APEGs maintain their shape in air, as shown in Figure S14, Supporting Information. The 3D printed APEGs also show pH responsive behaviors by dissolving shellac NPs under alkaline condition[35] and thus breaking the network of bridged water droplets, as shown in Figure S15, Supporting Information.

The strategy of preparing APEGs is applicable to various systems, which are excellent candidates for the preparation of APEG-templated functional materials. The mechanical properties of the materials prepared by photopolymerizing the APEG systems are tunable by adjusting the concentrations of monomers and cross-linkers (CL), which are characterized in detail in Table S1, Supporting Information. When mixtures of styrene (St) monomer, a stiff and brittle material with a high T_g, and *n*-butyl acrylate (BA) monomer, a soft and ductile material with a low T_g, are chosen as the model oil phases, the tensile modulus and tensile strength decrease, while strain at break increases when the St concentration decreases, as shown in Figure 4e,f. The cross-linking density is another control to tailor the mechanical properties of APEG-templated materials, as shown in Figure 4g; the materials with lower cross-linking density demonstrate lower tensile modulus, lower tensile strength, and higher strain at break. Therefore, 3D printing of APEG systems provides a facile platform for the development

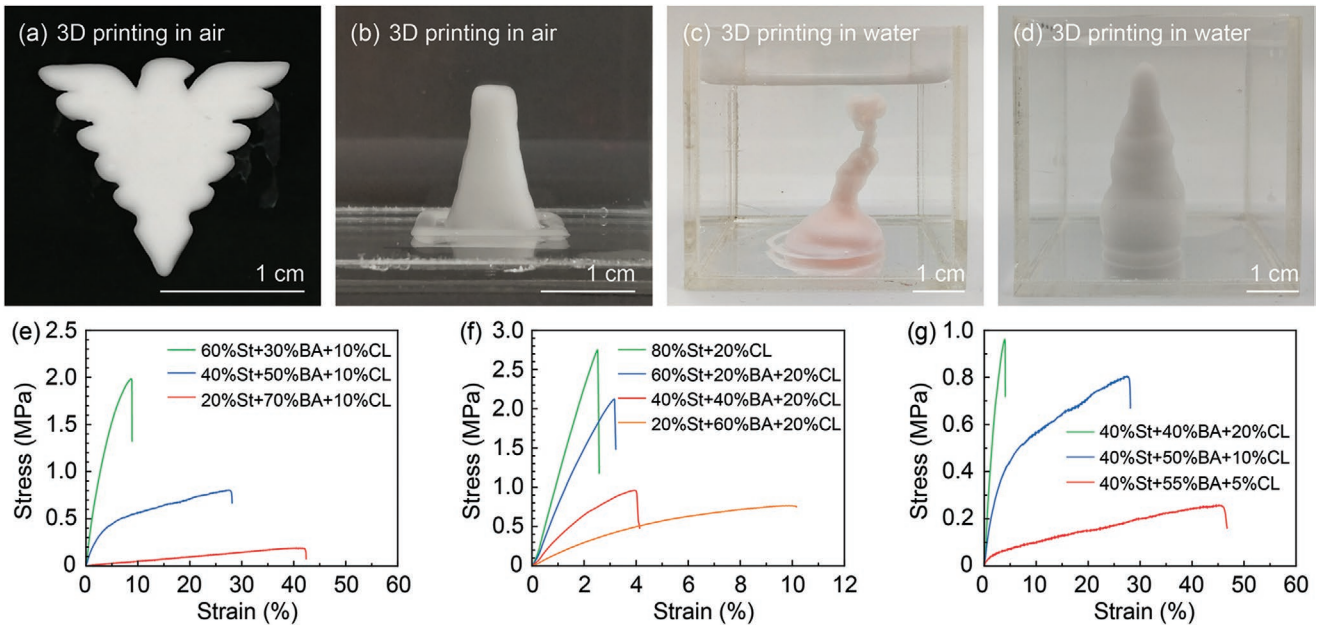

Figure 4. 3D printing of APEGs under different conditions and preparation of APEG-templated materials with tunable mechanical properties. a,b) 3D printing of APEGs in air. c,d) Underwater construction of 3D models by directly printing APEGs in water. e–g) Tuning the mechanical performances of APEG-templated porous materials by adjusting the concentrations of styrene (St) monomers, *n*-butyl acrylate (BA) monomers, and cross-linkers (CL). The CL are trimethylolpropane acrylate and ethylene glycol dimethacrylate mixed at a volume ratio of 1:1. Because NH_2-PDMS-NH_2 is barely soluble in St and BA monomers, NH_2-PS-NH_2, which is synthesized by atom transfer radical polymerization and nucleophilic substitution reaction, is used in the systems.

of functional materials with customizable shapes and tunable mechanical properties.

2.5. APEG-Templated Thermal Insulation Materials

APEG-templated materials are naturally porous and are excellent candidates for thermal insulation materials. The pore size is controlled by the shear strength, which produces water droplets of different sizes, and the porosity is tuned by adjusting the volume fraction of water droplets. Interestingly, both closed or open cell microstructure of APEG-templated materials can be achieved. To demonstrate this, BA monomer is chosen as the model oil phase and porous polybutyl acrylate (PBA) materials with closed or open cells are prepared using APEGs as templates. When the photoinitiator, lithium phenyl(2,4,6-trimethylbenzoyl)phosphinate, is added in the water phase, photolysis takes place in the water droplets under UV irradiation. As the radicals diffuse toward the water/oil interface, the polymerization of BA monomers immediately initiates, forming a thin dense film at the interface and leading to closed cells, as shown in **Figure 5**a and modeled in Figure 5b. Alternatively, when the photoinitiator, phenylbis(2,4,6-trimethylbenzoyl)phosphine oxide, is added in the oil phase, initiation and polymerization start in the oil phase and lead to temperature and concentration gradients during the polymerization process. The gradients then could result in interfacial instability and cause the thin oil layers between neighboring water droplets to rupture,[36] forming interconnected open cells, as shown in Figure 5c and modeled in Figure 5d.

To test the performances of APEG-templated thermal insulation materials, we compare the surface temperature of porous PBA with closed cells, porous PBA with open cells, dense PBA and commercial thermal insulation foam with the same thickness on a hot stage using a thermal imager, as shown in Figure 5e. The results reveal that porous PBA with open cells demonstrates the largest temperature difference between the hot plate surface and the material surface. In addition, porous PBA with open cells shows smaller fluctuations of surface temperature than that of commercial thermal insulation foam, which is attributed to the uniform porous microstructure of APEG-templated materials.

3. Conclusions

Attractive Pickering emulsion gels are designed by engineering interdroplet interactions at molecular scale via the electrostatic interactions between carboxyl functionalized nanoparticles in the dispersed water droplets and α,ω-diamino functionalized telechelic polymers in the continuous oil phase. The strategy of preparing APEGs is applicable to various systems and the

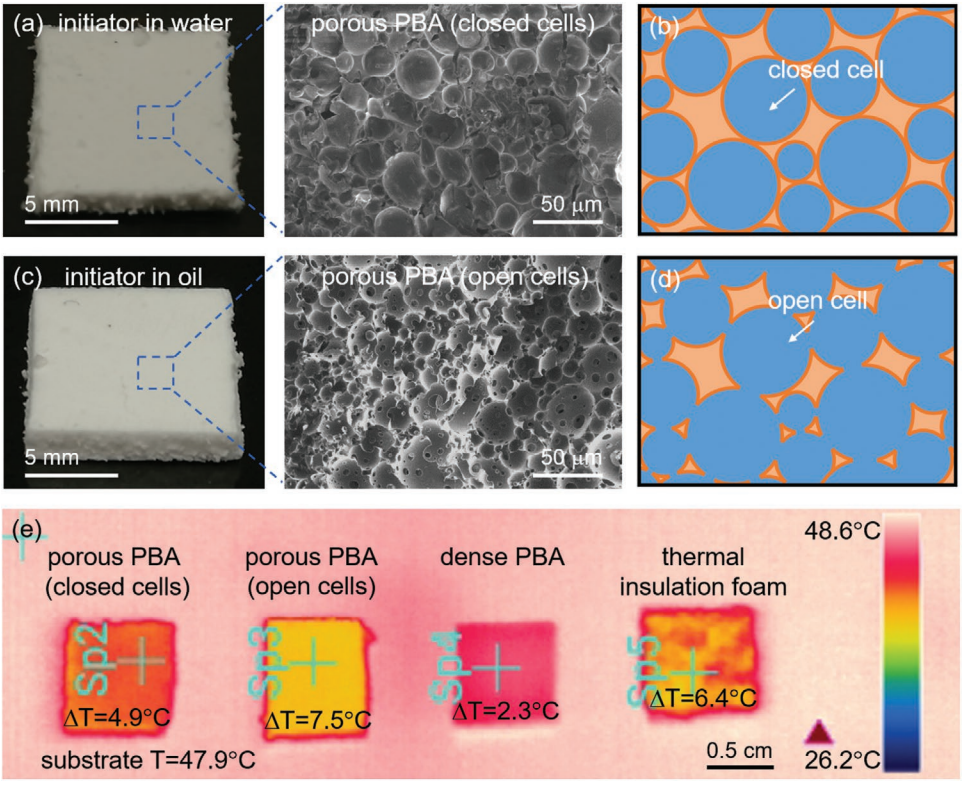

Figure 5. Porous thermal insulation materials prepared using APEGs as templates. a) Porous polybutyl acrylate (PBA) materials with closed cells prepared with initiator in water and modeled in b). c) Porous PBA materials with open cells prepared with initiator in oil and modeled in d). e) Thermal insulation performances of porous PBA with closed cells, porous PBA with open cells, dense PBA and thermal insulation foam. "+" indicates the spot where the temperature is measured. Sp2, Sp3, Sp4, and Sp5 denote the sampling spots on the surface of porous PBA with closed cells, porous PBA with open cells, dense PBA and thermal insulation foam, respectively.

network of water droplets bridged by telechelic polymers shows typical shear-thinning behaviors. The unique viscoelastic properties of the APEG systems make APEGs ideal for 3D printing inks, which enable the facile processing and customized design of functional materials by direct 3D printing in air and under water. The 3D-printed architectures can further be photopolymerized to achieve APEG-templated materials. By controlling the photopolymerization process, APEG-templated thermal insulation materials with open cells are achieved, which show better performance than commercial thermal insulation foam. The APEGs are versatile and provide an excellent platform for customized design of functional materials with desired shapes, tunable properties, and optimized performances.

Supporting Information

Supporting Information is available from the Wiley Online Library or from the author.

Acknowledgements

B.W., C.Y., and Q.X. contributed equally to this work. This work was supported by the National Natural Science Foundation of China (Grant Nos. 21878258, 81874173, 82074208, and 81472346), Zhejiang Provincial Natural Science Foundation of China (Grant No. Y20B060027), and Zhejiang University Education Foundation Global Partnership Fund. This work was also supported by the National Science Foundation (No. DMR1310266) and the Harvard Materials Research Science and Engineering Center (No. DMR-1420570). B.W. acknowledges the financial support from the China Postdoctoral Science Foundation (No. 2019TQ0274).

Conflict of Interest

The authors declare no conflict of interest.

Data Availability Statement

Research data are not shared.

Keywords

3D printing, emulsion gels, pickering emulsions, porous materials, shear thinning

Received: March 26, 2021
Revised: May 1, 2021
Published online:

[1] E. Dickinson, *Food Hydrocolloids* **2012**, *28*, 224.
[2] L. Xiao, Z. Wang, Y. Sun, B. Li, B. Wu, C. Ma, V. S. Petrovskii, X. Gu, D. Chen, I. I. Potemkin, A. Herrmann, H. Zhang, K. Liu, *Angew. Chem., Int. Ed.* **2021**, *60*, 12082.
[3] A. Kogan, N. Garti, *Adv. Colloid Interface Sci.* **2006**, *123*, 369.
[4] B. Wu, C. Yang, B. Li, L. Feng, M. Hai, C.-X. Zhao, D. Chen, K. Liu, D. A. Weitz, *Small* **2020**, *16*, 2002716.
[5] Z. Hu, T. Patten, R. Pelton, E. D. Cranston, *ACS Sustainable Chem. Eng.* **2015**, *3*, 1023.
[6] D. Bais, A. Trevisan, R. Lapasin, P. Partal, C. Gallegos, *J. Colloid Interface Sci.* **2005**, *290*, 546.
[7] J. T. Muth, P. G. Dixon, L. Woish, L. J. Gibson, J. A. Lewis, *Proc. Natl. Acad. Sci. USA* **2017**, *114*, 1832.
[8] Y. Luo, Q. Wang, J. Li, F. Xu, L. Sun, Y. Zou, H. Chu, B. Li, K. Zhang, *Mater. Today Nano* **2020**, *9*, 100071.
[9] T. Farjami, A. Madadlou, *Trends Food Sci. Technol.* **2019**, *86*, 85.
[10] T. Sheth, S. Seshadri, T. Prileszky, M. E. Helgeson, *Nat. Rev. Mater.* **2020**, *5*, 214.
[11] C. Huang, J. Forth, W. Wang, K. Hong, G. S. Smith, B. A. Helms, T. P. Russell, *Nat. Nanotechnol.* **2017**, *12*, 1060.
[12] X. Chen, K. Liu, P. He, H. Zhang, Y. Fang, *Langmuir* **2012**, *28*, 9275.
[13] J. Li, B. Li, J. Sun, C. Ma, S. Wan, Y. Li, R. Göstl, A. Herrmann, K. Liu, H. Zhang, *Adv. Mater.* **2020**, *32*, 2000964.
[14] V. V. Erramreddy, S. Ghosh, *Colloid Surf. A* **2015**, *484*, 144.
[15] V. O. Ikem, A. Menner, A. Bismarck, *Angew. Chem., Int. Ed.* **2008**, *47*, 8277.
[16] R. Butler, C. M. Davies, A. I. Cooper, *Adv. Mater.* **2001**, *13*, 1459.
[17] T. G. Mason, J. Bibette, D. A. Weitz, *Phys. Rev. Lett.* **1995**, *75*, 2051.
[18] M. E. Helgeson, S. E. Moran, H. Z. An, P. S. Doyle, *Nat. Mater.* **2012**, *11*, 344.
[19] M. Filali, M. J. Ouazzani, E. Michel, R. Aznar, G. Porte, J. Appell, *J. Phys. Chem. B* **2001**, *105*, 10528.
[20] H. Tsurusawa, S. Arai, H. Tanaka, *Sci. Adv.* **2020**, *6*, eabb8107.
[21] S. M. Hashemnejad, A. Z. M. Badruddoza, B. Zarket, C. R. Castaneda, P. S. Doyle, *Nat. Commun.* **2019**, *10*, 2749.
[22] L. Kong, R. Chen, X. Wang, C.-X. Zhao, Q. Chen, M. Hai, D. Chen, Z. Yang, D. A. Weitz, *Lab Chip* **2019**, *19*, 2089.
[23] Z. Sun, C. J. Yang, F. Wang, B. H. Wu, B. Q. Shao, Z. C. Li, D. Chen, Z. Z. Yang, K. Liu, *Angew. Chem., Int. Ed.* **2020**, *59*, 9365.
[24] B. P. Binks, R. Murakami, *Nat. Mater.* **2006**, *5*, 865.
[25] C. Huang, Y. Chai, Y. Jiang, J. Forth, P. D. Ashby, M. M. L. Arras, K. Hong, G. S. Smith, P. Yin, T. P. Russell, *Nano Lett.* **2018**, *18*, 2525.
[26] J. Forth, X. Liu, J. Hasnain, A. Toor, K. Miszta, S. Shi, P. L. Geissler, T. Emrick, B. A. Helms, T. P. Russell, *Adv. Mater.* **2018**, *30*, 1707603.
[27] C. Ma, J. Dong, M. Viviani, I. Tulini, N. Pontillo, S. Maity, Y. Zhou, W. H. Roos, K. Liu, A. Herrmann, G. Portale, *Sci. Adv.* **2020**, *6*, eabc0810.
[28] M. Costantini, J. Guzowski, P. J. Żuk, P. Mozetic, S. De Panfilis, J. Jaroszewicz, M. Heljak, M. Massimi, M. Pierron, M. Trombetta, M. Dentini, W. Święszkowski, A. Rainer, P. Garstecki, A. Barbetta, *Adv. Funct. Mater.* **2018**, *28*, 1800874.
[29] Z. Zhao, Y. Liu, K. Zhang, S. Zhuo, R. Fang, J. Zhang, L. Jiang, M. Liu, *Angew. Chem., Int. Ed.* **2017**, *56*, 13464.
[30] Y. Farag, C. S. Leopold, *Dissolution Technol.* **2009**, *16*, 33.
[31] S. R. Bhatia, W. B. Russel, *Macromolecules* **2000**, *33*, 5713.
[32] C. Yang, B. Wu, J. Ruan, P. Zhao, L. Chen, D. Chen, F. Ye, *Adv. Mater.* **2021**, *33*, 2006361.
[33] D. W. Johnson, C. Sherborne, M. P. Didsbury, C. Pateman, N. R. Cameron, F. Claeyssens, *Adv. Mater.* **2013**, *25*, 3178.
[34] G. Liu, Y. He, P. Liu, Z. Chen, X. Chen, L. Wan, Y. Li, J. Lu, *Engineering* **2020**, *6*, 1232.
[35] L. Kong, X. Jin, D. Hu, L. Feng, D. Chen, H. Li, *Chin. Chem. Lett.* **2019**, *30*, 2351.
[36] I. Gurevitch, M. S. Silverstein, *Macromolecules* **2012**, *45*, 6450.